



# Ultra-fast MRI of the human brain with simultaneous multi-slice imaging

David A. Feinberg<sup>a,b,c,\*</sup>, Kawin Setsompop<sup>d,e</sup>

<sup>a</sup> Helen Wills Institute for Neuroscience, University of California, Berkeley, CA, USA

<sup>b</sup> Advanced MRI Technologies, Sebastopol, CA, USA

<sup>c</sup> Department of Radiology, University of California, San Francisco, USA

<sup>d</sup> Athinoula A. Martinos Center for Biomedical Imaging, Department of Radiology, Massachusetts General Hospital, Charlestown, MA, USA

<sup>e</sup> Harvard Medical School, Boston, MA, USA

## ARTICLE INFO

### Article history:

Received 25 September 2012

Revised 28 January 2013

Available online 13 February 2013

### Keywords:

Echo planar

MRI

EPI

GRASE

Simultaneous multi-slice

Multiband

MB

EVI

GRAPPA

Functional connectivity

Connectome

fMRI

Diffusion

Fiber tractography

Fast imaging

Parallel imaging

fMRI

BOLD

Multiplexed-EPI

Simultaneous Multi-Slice EPI

Blipped-CAIPI

## ABSTRACT

The recent advancement of simultaneous multi-slice imaging using multiband excitation has dramatically reduced the scan time of the brain. The evolution of this parallel imaging technique began over a decade ago and through recent sequence improvements has reduced the acquisition time of multi-slice EPI by over ten fold. This technique has recently become extremely useful for (i) functional MRI studies improving the statistical definition of neuronal networks, and (ii) diffusion based fiber tractography to visualize structural connections in the human brain. Several applications and evaluations are underway which show promise for this family of fast imaging sequences.

© 2013 Elsevier Inc. All rights reserved.

## 1. The brain is the challenge

It is hard to comprehend the daunting scale of neuronal networks let alone the number of neurons in the human brain. It is known that the human cerebral cortex contains  $\sim 10^{10}$  neurons and  $\sim 10^{14}$  synaptic connections therefore mapping this neuronal network on its smallest “micro” scale is currently an impossible task. On a macro-scale, the human brain is structurally organized into the cerebral cortex, the highly cellular gray matter in a convoluted sheet  $\sim 3$  mm thick, covering  $\sim 1000$  cm<sup>2</sup> and folded into gyri in each of two hemispheres [1]. The cortex has distinct functional

areas which have underlying connecting white matter fiber tracks, nevertheless the number of different cortical areas, their boundaries and long range fiber connectivity have not been completely defined. It has been proposed that there are  $\sim 150$ – $200$  cortical areas with distinct neuronal function, connectivity and network organization [2]. Efforts are underway to use MRI for large scale mapping of the normal human brain [3] and to use high resolution MRI to study cortical organization at an intermediate scale. Using cortical layer specific resolutions, it is possible to study neuronal circuit inputs and outputs to different cortical layers as well as different cortical functional organization [4–6]. Previously described anatomically and functionally distinct neuronal populations forming local circuits into distinct subunits, i.e. cortical columns [7] have been identified with functional MRI (fMRI) [8].

\* Corresponding author at: Helen Wills Institute for Neuroscience, University of California, Berkeley, CA, USA.

E-mail address: [david.feinberg@berkeley.edu](mailto:david.feinberg@berkeley.edu) (D.A. Feinberg).

The long measurement time of MRI has hampered large scale mapping of structural and functional connectivity in the brain for which both higher spatial and temporal resolutions are critical for the task. In this review we focus on advances in fast MRI imaging recently being used for neuronal network mapping. To study brain circuitry and functional organization, several different approaches exist including task based fMRI, resting state fMRI and diffusion based axonal fiber tractography. The term ‘resting state fMRI’ is a misnomer since the brain is actually quite active in functional connectivity studies. The subject lies awake with no stimulus or task, while the fMRI scans the entire brain in hundreds or thousands of times to detect spontaneous brain activity occurring in different cortical areas for which strong correlation in activity indicates areas are connected in networks with functional connectivity. Diffusion imaging is a very different approach to identify brain connectivity through 3D fiber reconstructions utilizing anisotropic characteristics encoded in diffusion images [9,10] revealing neuronal fiber orientations and pathways.

We will review recent imaging sequences utilizing simultaneous and multiplexed signal encodings. The faster diffusion imaging is useful to achieve higher spatial and angular resolutions in fiber tractography [11]. And use of these faster imaging sequences recently led to the discovery how faster BOLD sampling of the brain greatly improves the statistical definition of functional connectivity networks between different cortical regions [12]. We give our perspective on the very recent advances in simultaneous multi-slice imaging, now very much faster than EPI and with such sub-second whole brain MRI underpinning recent neuroscience research.

### 1.1. Echo planar imaging is the workhorse

Echo planar imaging (EPI) [13,14] with its extremely high sensitivity to blood susceptibility contrast mechanisms and its extremely fast “snap-shot imaging” speed is used for nearly all fMRI studies [15,16]. The single echo train of EPI is critically important for successful fMRI and diffusion imaging due to smoothly varying velocity dependent phase shifts through the echo train, whereas the phase errors become discontinuous or periodic in multi-shot imaging sequences. The single-shot EPI phase error function in  $k$ -space avoids ghost artifacts from pulsatile CSF and brain velocity [17] that can obscure the low level signal. Single-shot EPI is also the most commonly used pulse sequence for diffusion imaging of human brain, producing 3D data for visualization of neuronal fiber tractography. Diffusion imaging with high angular resolution (HARDI) schemes may show exquisitely beautiful patterns of neuronal fibertracks [18], however, they can take over 10 h in ex vivo animal studies and such times are intolerable in human studies.

For the last few decades, the acquisition time of EPI images used for fMRI and diffusion imaging not been substantially reduced. Nearly all efforts to make EPI faster have depended on shortening the echo train time both by reducing the number of echoes and through faster gradient switching with the goal to reduce  $T_2^*$  signal decay and image artifacts. These include partial Fourier [19], parallel imaging [20,21] and gradient ramp sampling and sparse sampling techniques [22]. While these techniques significantly reduce the echo train period, they do not reduce the initial sequence time used to encode diffusion or blood oxygen level dependent (BOLD) fMRI contrast. With incorporation of partial Fourier and parallel imaging into EPI, scan times for imaging the entire brain have decreased by less than half for fMRI and very little for diffusion imaging. Nonetheless, these techniques have benefits of reducing artifacts, image distortions from field inhomogeneity and in raising signal by reducing the effective TE, the echo time encoding the center of  $k$ -space. In particular, for diffusion imaging,

the shorter TE reduces  $T_2$  signal decay and therefore compensates for SNR reduced by the square root of the acceleration factor [23].

The optimal encoding time for BOLD contrast is dependent on field strength by  $TE = \sim T_2^*$ , but with trade-offs in reduced SNR at later TE, hence at 7 Tesla (T) the optimal TE for fMRI ranges from 15 to 25 ms and for fMRI at 3 T ranges from 30 to 40 ms. With shorter TE the trade-off exist between reduced BOLD contrast and higher SNR and less signal drop-out artifact in brain near regions of air sinuses or bone interfaces with high susceptibility. In diffusion imaging the diffusion sensitizing period usually ranges between 20 and 100 ms depending on the amount of diffusion encoding ( $b$ -value). This is determined by the gradient system’s maximum gradient amplitude which ranges from 30 to 50 mT/m on most human scanners. These contrast encoding times cannot be shortened without reducing the desired physiologic contrast of BOLD or diffusion in images. The duration of EPI echo trains vary upon several factors particularly image resolution, parallel imaging and partial Fourier reductions, however echo train times are typically between 20 and 80 ms, on the time scale of the physiological encodings, hence the total time of the pulse sequence cannot be reduced too greatly. For fMRI studies, the time constraints of conventional EPI impose a restriction on the ability to acquire very high-resolution whole brain image in a time frame suitable for typical fMRI paradigms (<3 s); for example, 1 mm isotropic whole brain acquisition with  $\sim 100$  imaging slices would result in a TR of 8–9 s. As above, higher spatial resolution was a strong driving force in the first applications of SMS-EPI to fMRI at [24] and to reduce the long acquisition time of diffusion imaging [11,12].

In general, it is extremely inefficient to spend time encoding diffusion contrast or BOLD contrast in all brain regions but then to only read out one slice. To significantly shorten the diffusion and fMRI scan times, the initial diffusion gradients or the  $T_2^*$  BOLD period in a pulse sequence can encode several images in the same sequence rather than only one image. To do this, there are at least three ways to encode multiple 2D images in a single-shot pulse sequence. What will be the major topic of this review, first is a slice variant of parallel imaging with which it is possible to perform simultaneous multi-slice imaging [25]. A second approach is to use multiple excitation pulses to refocus echoes from different images in an echo train known as simultaneous image refocused (SIR) EPI [26] (knighting EPI to match Sir Peter Mansfield). Third, is to perform single-shot 3D imaging sequences by modulating gradients on two spatial axes in addition to the frequency readout axis to achieve 3D spatial encoding, with the earliest method being echo volume imaging by Mansfield [13,27]. In EVI or more recent 3D imaging sequences, the entire image volume is inherently encoded by an initial contrast labeling period in the sequence. In this review, we will focus on the first two approaches, which have seen dramatic development over the last few years.

### 1.2. Simultaneous multi-slice EPI

The simultaneous multi-slice (SMS) pulse sequence applies a multiband (MB) composite RF pulse with slice-selective gradient to simultaneously excite multiple slice planes. With standard 2D  $k$ -space encoding alone, the images from simultaneously excited slices are not distinguishable. Nonetheless, the use of an RF receive coil array can provide the extra spatial encoding that will allow these images to be separated. David Larkman and colleagues at Imperial College first proposed and demonstrated simultaneous multi-slice MRI utilizing multiple RF coils and SENSE image reconstruction to separate simultaneously acquired imaging slices [25].

The SMS imaging can be formulated in image domain with SENSE reconstruction as:

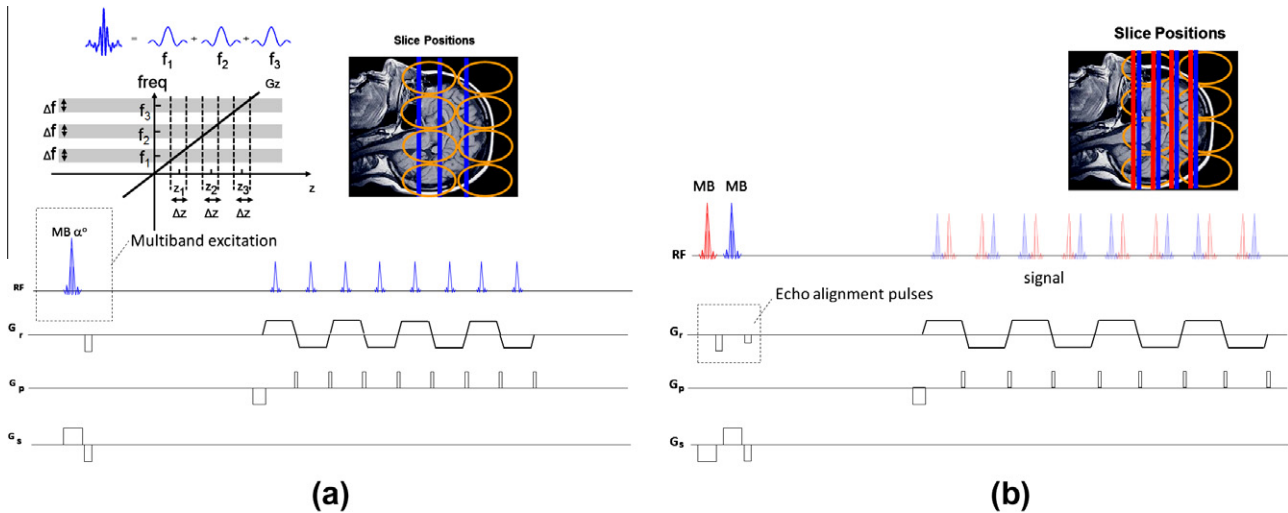


**Fig. 1.** Pulse sequence diagrams comparing variations of (a) simultaneous multi-slice (SMS) EPI and (b) multiplexed EPI with MB  $\times$  SIR images per echo train. Diagram shows (a) simultaneous excitation with a multiband pulse of 3 slice planes with sinc modulated rf pulses to excite different bands on the slice selective gradient axis. The signals of the slices are superimposed in the echo train and separated with information from different rf coils requiring sensitivity profiles by acquiring the slices separately. (b) Multiplexed EPI using SIR  $\times$  MB encoded images. The sequence uses multiple MB excitation pulses with small interposition gradient pulses on Gr axis to shift the respective echoes onto two halves of each readout time period, with each gradient reversal simultaneously refocusing echoes into an echo train. The echoes are sorted into two different k-spaces before performing slice GRAPPA extraction of their corresponding SMS images.

$$S_{i1}x_1 + S_{i2}x_2 + \dots + S_{ij}x_j + \dots + S_{im}x_m = C_i$$

where  $S_{ij}$  is the complex sensitivity of coil  $i$  at slice  $j$ , and  $x_j$  is the spatially dependent complex signal from slice  $j$ .  $C_i$  is the complex signal acquired in coil  $i$  in image domain. Hence through the use of sensitivity profiles (estimated via a separate set of single band images), the signal from each of the imaging slices can be estimated as  $[x] = [S]^{-1} \cdot [C]$  (Note: for improved reconstruction, information about the coils' noise covariance can be used to whiten/pre-process the signal C) [20,28].

The use of SMS in EPI and for human brain imaging was first demonstrated by Nunes et al. [29] where it was shown that high g-factor noise amplification is generally observed due to the typically smaller volume of coverage along the slice direction, Fig. 1. This smaller volume of coverage causes the distances between simultaneously excited slices and hence the aliasing voxel to be small; resulting in a poorly conditioned unaliasing reconstruction problem. A method to mitigate this issue based on the Wideband technique [30] was also proposed in this work, utilizing unipolar blipped gradient pulses on Gs concurrent with blipped phase encoding pulses on Gp, but this causes significant voxel blurring artifact. Moeller and colleagues at Minnesota used SMS-EPI for fMRI at 7 Tesla [24] to achieve a TR useful for fMRI studies while increasing the number slices made thinner to reduce through-plane dephasing from B0 inhomogeneity, problematic at ultra-high field imaging. In this work, the use of large coil array with improved spatial orthogonality of the coil elements at high field strength plays an important role to partially mitigate the g-factor penalty issue. Moeller utilized a SENSE/GRAPPA hybrid approach proposed by Blaimer et al. [31] to implement the reconstruction for the SMS acquisition. Studies performed at 7 T were in coronal plane to take advantage of the larger coil numbers along that imaging plane to achieve MB-4 using a 24 channel coil [24]. A point about nomenclature is that multiband (MB) and 'simultaneous multi-slice' (SMS) have recently been used interchangeably in the literature. Here we maintain the earliest name hence SMS-EPI, while utilizing the term MB to describe slice acceleration factors created by the multiband pulses e.g. MB-4.

### 1.3. Simultaneous image refocused (SIR) EPI

Concurrent with the early work by Larkman, a different approach of simultaneous echo train imaging was described [26] as *simultaneous image refocused* (SIR) EPI or *simultaneous echo refocused* (SER) EPI. A major difference from SMS is that SIR EPI does not use parallel imaging and coil sensitivity for image separation. Instead it applies sequentially two or more excitation pulses to create separable signals from two or more slices, Fig. 1b. The SIR method relies on defocusing pulses on Gr axis placed between the excitation pulses to modify the refocusing times of echoes from different slices. Dissimilar to SMS where echoes from different slices are concurrent, SIR separates slice echoes in each read period of the echo train. Therefore the ability to separate SIR-EPI slices is not dependent on coil sensitivity so slices can be acquired contiguously adjacent at small distances without suffering directly from g-factor related SNR losses. SIR technique has increased image distortion from larger echo spacing and inherent to EPI will have signal loss in regions of high susceptibility.

Reduction in scan time is extremely valuable for diffusion imaging, which can otherwise exceed human tolerance. The shortening of scan time allows larger data sets for higher spatial resolution angular resolution to be used. SIR-EPI was the earliest method to significantly reduce the TR and the acquisition time of high angular resolution diffusion imaging (HARDI). The relatively large sequence time for diffusion encoding effects several SIR slices simultaneously, rather than a single slice, for greater efficiency [32]. Fig. 3 shows the fiber tracks from diffusion imaging acquisitions comparing normal EPI to SIR-2 EPI and SIR-3 EPI, with the acquisition time reduced from 25 min to 8.5 min. The disadvantage of using SIR-EPI in diffusion imaging is the delay in TE by as much as 10–15 ms which reduces SNR and can only be mitigated by incorporation of partial Fourier and in-plane parallel imaging techniques.

Unlike diffusion imaging which favors the earliest possible TE to maximize signal following the diffusional signal loss, in fMRI a later TE is desirable for greater T2\* dependent BOLD contrast, and therefore a sequence dead time of 10–20 ms is often used before the echo train readout. This delay time can be replaced with the lengthened echo train in SIR EPI for efficient use of total acquisition

time without lengthening of TE. However for high spatial resolution acquisition (below 2 mm), SIR requires longer echo trains and in effect compound the TE delay.

#### 1.4. Multiplexed-EPI combines SIR and SMS

Combining the two orthogonal acceleration approaches produced what is referred to as multiplexed EPI [12,33]. The slice acceleration factor of multiplexed EPI is given by the product of the accelerations of SIR and MB, resulting in a net number of images per echo train =  $SIR \times MB$  as shown in Fig. 2. Maximum acceleration factor of  $4 \times 3 = 12$  slices was demonstrated [12] but was limited by image g-factors and artifact from SMS-EPI. Image artifacts from higher g-factor can be observed with  $MB = 3$  and image distortions become more severe. Fig. 4 shows functional connectivity in human brain has improved definition with multiplexed-EPI allowing faster TRs of .4s and .8s compared to 2.5s using normal EPI. The greater precision in the temporal sam-

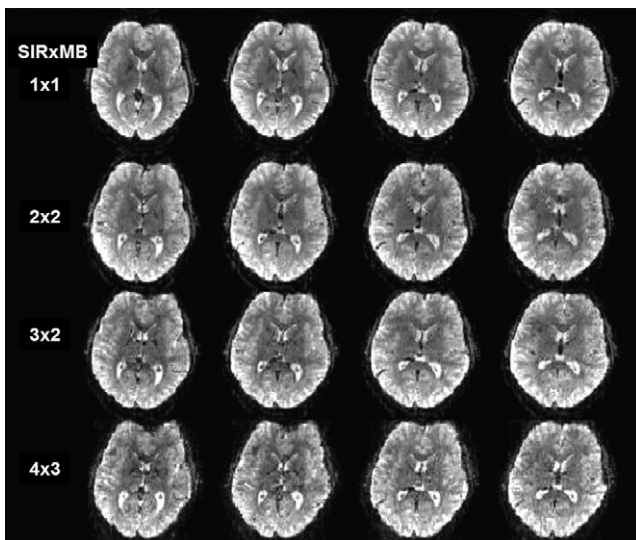


**Fig. 2.** Comparison of multiplexed EPI images at different acceleration factors. Each row shows 4 adjacent slices out of total 60 slices at 2 mm isotropic resolution covering the entire brain. Each row of images was obtained with a different pulse sequence and slice acceleration ( $SIR \times MB$ ) producing 1, 4, 6 and 12 slices from the EPI echo train. Maximum MB acceleration was limited to 3 due to artifacts from large g-factors as the sequence did not use blipped-CAIPI controlled aliasing. SIR factor was limited by increased distortions. Adapted from [12].

pling of the slowly varying spontaneous BOLD signal resulted in improved resolution of functional networks. For gradient echo sequence with acquisition performed at the Ernst angle, the SNR per shot will decrease, while the SNR per unit time will increase as TR is reduced (assuming thermal noise dominates).

SMS and SIR can be used to considerably speed up fMRI and diffusion acquisitions, but important trade-offs have to be considered. For fMRI using SMS-EPI, a shorter TR results in higher temporal sampling rate, which increases SNR per unit time until this gain is offset by the higher g-factors and signal loss from reduced T1 recovery. Reductions in SNR due to in-plane slice accelerations are well known [24,34]. For many fMRI protocols, physiological noise is the dominating noise source, thereby the g-factor penalty and image thermal noise is less crucial and a higher MB acceleration factor can be utilized. Using SIR in multiplexed EPI further increases acquisition speed and number of images per echo train, however, SIR increases the total echo readout time and echo spacing which increases geometric distortions, signal dropout, and minimum achievable TE. By efficient use of gradient ramp sampling and with the read gradient switching being shared to form multiple echoes, SIR-2 is ~35% longer time than EPI and SIR-3 is ~80% longer, not double or triple the time, when using 40 mT/m maximum gradients and pulse durations for 2.5 mm isotropic spatial resolution useful for fMRI. It is also possible to incorporate in-plane parallel imaging to reduce the effective echo spacing and echo train length (N) by half or more, however, the reduced geometric distortions are at a price of higher g-factor and  $\sqrt{N}$  SNR loss. With higher MB-factor in SMS EPI, the increased g-factor has a heterogeneous distribution in each different image depending on the coil array geometry. Quite dissimilar, SIR does not use coil sensitivity profiles to separate images so images can be adjacent to each other without increasing g-factor.

#### 1.5. Controlled aliasing improves SMS-EPI and makes it several times faster

The concept of hexagonal sampling was introduced to the signal processing [35] and further ideas were proposed to MRI [36,37] to control the aliasing pattern and improve upon de-aliasing of conventional rectangular sampling. Such approaches first found their use in MRI to spatial-temporal sampling efficiency [38]. The ability for SMS technique to accelerate the EPI acquisition is limited by the ill-conditioning of parallel imaging reconstruction at high slice acceleration factors. The “controlled aliasing in parallel imaging results in higher acceleration” (CAIPIRINHA) technique was proposed by the Wurzburg group [39] to mitigate this issue by introducing

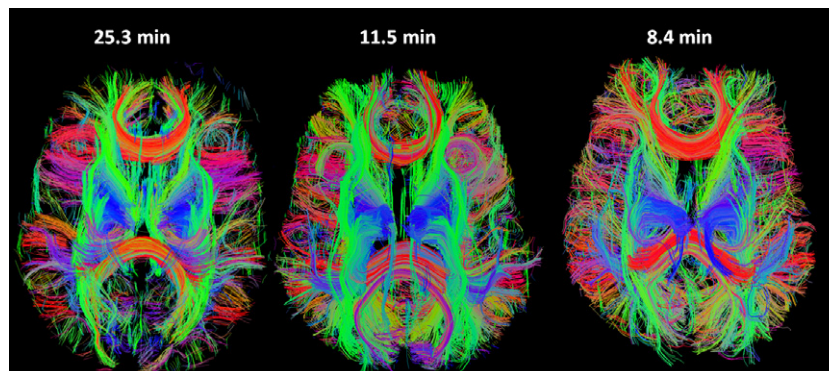


**Fig. 3.** Diffusion imaging for neuronal fiber track display accelerated with simultaneous image acquisition. The 3D images show neuronal axon fiber tracks in the human brain, in vivo, using simultaneous image refocused (SIR) EPI with either 2 or 3 images per echo train. Compared to EPI (left) the full 3D data set was acquired 2–3 times faster with SIR-2 EPI (center) and SIR-3 EPI (right) with acquisition times shown. The fibertrack images were not exactly aligned and small differences in distortion are present. The colors designate direction of fibers in orthogonal axes. Adapted from [67].

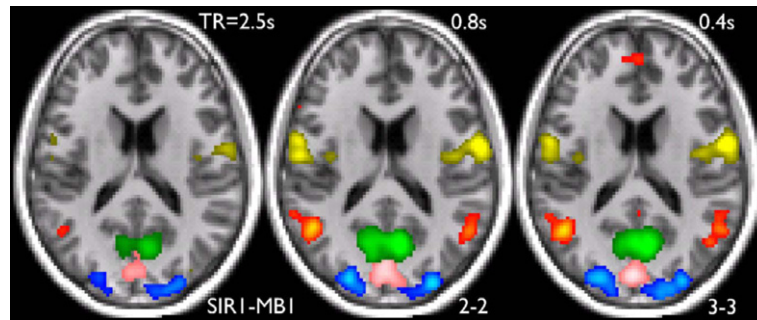


**Fig. 4.** Faster imaging improves statistical definition of networks in functional connectivity maps. Functional connectivity determined by the correlation of BOLD activity occurring throughout the entire brain. Here an axial image showing four networks in different colors. The networks have higher statistical significance to show larger color areas using higher sampling rates comparing (left to right) normal EPI, 4 images per echo train, and 9 images per echo train using multiplexed EPI for TR reduced from 2.5 s to 0.8 and 0.4 s, respectively. Adapted from [12]. (For interpretation of the references to color in this figure legend, the reader is referred to the web version of this article.)

an in-plane image shift between the simultaneously acquired slices to increase the distance between aliasing voxels thereby making them easier to separate. This in plane shift was achieved by modulating the phase of the magnetization excited in the individual slices for each  $k$ -space line through using a different phase modulated RF pulse for each  $k$ -space line acquisition. For example, alternating the phase of every other  $k$ -space line's excitation by  $\pi$  will result in a spatial shift of FOV/2 in the PE direction for that slice. This concept was presented early on in the development of SMS imaging and precedes the work on SMS-EPI in [28,29].

Single-shot EPI uses only a single excitation pulse, preventing the use of CAIPIRINHA with RF pulse phase cycling to create the desired controlled aliasing. Alternative approach of incorporating controlled aliasing, suitable to EPI, was proposed on the basis of the wideband method [40], to create relative in-plane shifts between the simultaneously acquired slices, both in the readout direction [29,30] and in the phase encoding direction [29]. Unfortunately this technique relies on the use of slice gradient to introduce phase modulation during the readout, causing a continuous accumulation of through-slice phase and resulting in considerable degree of voxel tilting on the slice axis hence blurring of in-plane resolution.

To accomplish controlled aliasing in EPI without the limitation imposed by voxel tilt blurring, the blipped-CAIPI acquisition scheme [33] was proposed, Fig. 5. Unlike the wideband based technique, in the blipped-CAIPI technique the gradient pulses are designed specifically to periodically refocus (“phase rewind”) the

through-slice phase accumulation to overcome the voxel tilting artifact. The blipped-CAIPI method applies slice axis gradient pulses (blipped  $G_s$ ) during the read gradient switching, simultaneous with the image phase encode pulses ( $G_p$ ) to create the desired phase modulation between the simultaneously excited slices. An example of a blipped-CAIPI acquisition scheme to create an inter-slice FOV/2 shift along the  $y$  direction between two simultaneously excited slices is shown in Fig. 6 (for the case where one of the excited slice is at iso-center). The pulse sequence scheme is shown on the left, where the amplitude of the  $G_s$  blips, are chosen to each create a phase accrual of magnitude  $\pi$  for the top excited slice. The resulting linear phase modulation along  $k_y$  for the top slice is shown on the right of the figure. This phase modulation causes a FOV/2 shift for the top-slice while, the bottom slice, which is at iso-center, sees no phase modulation and hence is not affected by the  $G_s$  encodes. The resulting aliased FOV/2 inter-slice shifted image is shown on right of figure. For the general case where neither of the simultaneously excited slices are at iso-center, the *relative* phase modulation between the slices caused by each of the  $G_s$  encodes is still  $\pi$ , and a simple post-processing step can be used to correctly align the aliased images [33]. The use of blipped-CAIPI significantly reduces g-factor noise and artifact level, particularly at high MB acceleration factors, Fig. 7. Good quality images at accelerations of MB-6 and higher. There is no severe signal loss in the image central regions for which it was not necessary to “align” blipped CAIPI pulses as recently reported [41] to achieve gradient moment nulling at the  $k_0$  (center of  $k$ -space) echo posi-

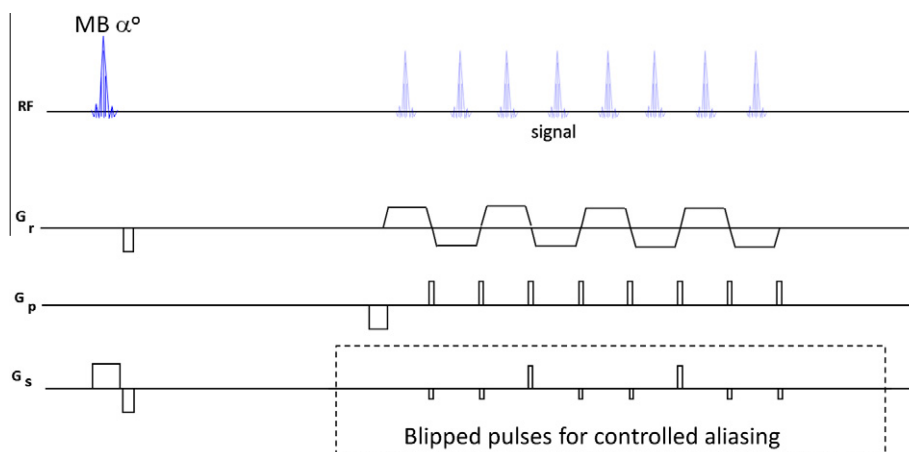


**Fig. 5.** SMS EPI blipped-CAIPI sequence modified with additional blipped gradient pulses (hatched box) with periodic gradient moment nulling with larger amplitude phase-rewind pulses to repeatedly null the gradient moment in the echo train. The particular 2 negative polarity blipped pulses followed by a 3rd positive polarity pulse to normalize the gradient moment and rewind net phase creates an FOV/3 controlled aliasing.

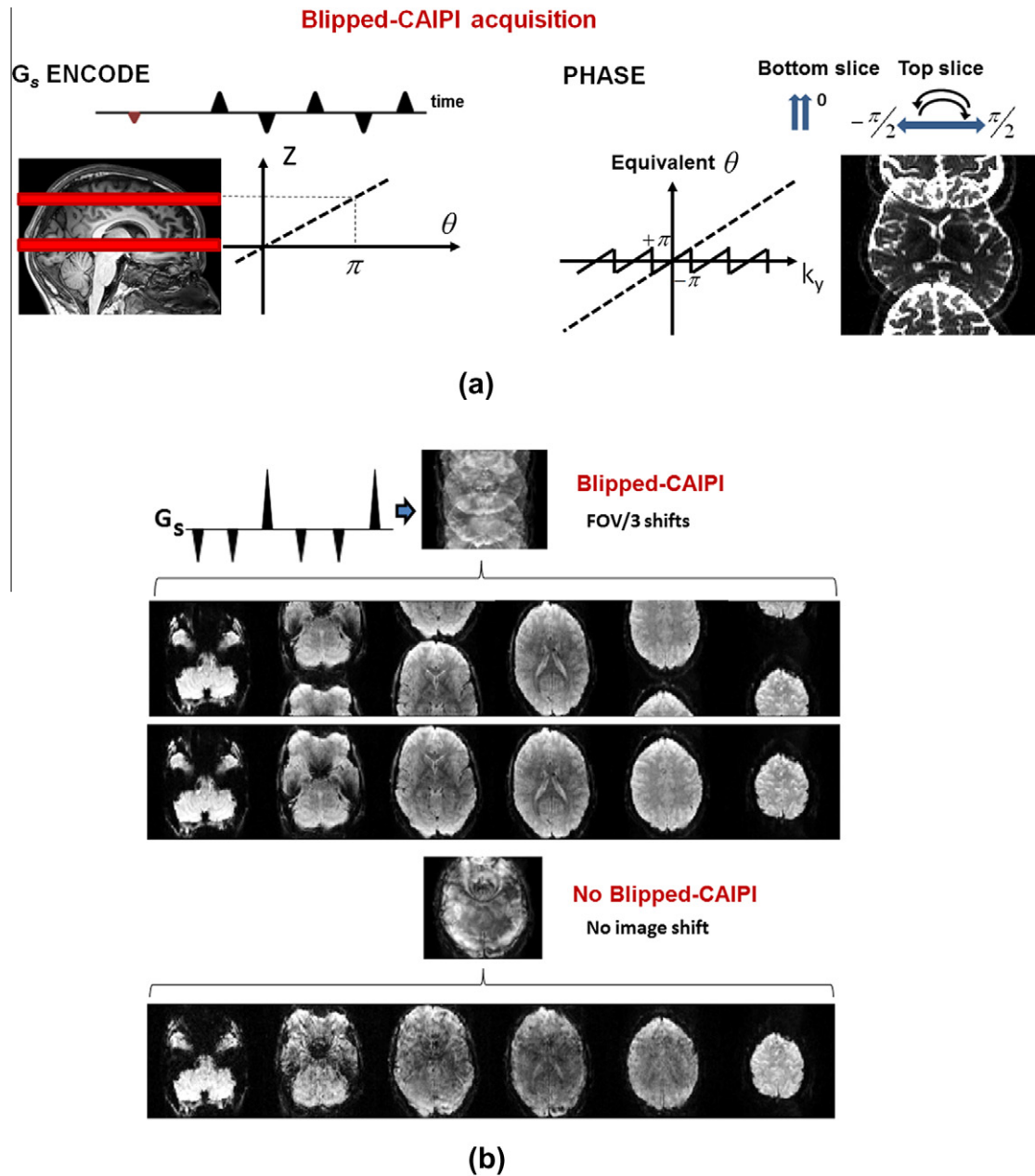


**Fig. 6.** (a) Provides details of the blipped-CAIPI acquisition scheme. The  $G_s$  gradient pulses shown are played out during the echo train readout and modulate the phase of the echoes as a function of slice position on the slice axis. The images become shifted in the field of view (FOV/2) on the phase encoded axis. Adapted from [11]. (b) Shown are FOV/3 inter-slice image shift in MB-6 simultaneous excited slices. The inter-slice shifted collapsed image is shown with its corresponding de-aliased images and final image process corrected images. Without blipped-CAIPI (bottom) there is superimposed alignment of the collapsed image data resulting in poorer image quality from image cross-talk and higher g-factor yielding lower SNR.

tion. There may however be reduced sensitivity to sources of encoding errors with the align approach, yet to be investigated.

The periodic reversal of the  $G_s$  gradient in the blipped-CAIPI sequence is the key to eliminate blurring artifact present in the wide-band technique which becomes prohibitively severe with closely spaced slices using higher MB factors. This periodic reversal significantly reduces the buildup of the gradient moment and the through-slice dephasing in the echo train. Additionally, the initial “balancing”  $G_s$  blip shown in red in the  $G_s$  encode scheme (Fig. 6a) can be used to further reduce minor ghosting artifact of the blipped-CAIPI sequence that is typically already very low.

For CAIPIRINHA based acquisitions, image domain based reconstruction via SENSE algorithm is directly applicable. However, a  $k$ -

space based reconstruction using the SENSE/GRAPPA hybrid technique [31] results in significant artifact. To overcome this issue the slice-GRAPPA reconstruction algorithm was proposed [33]. It uses a separate GRAPPA-like kernel set [21] to estimate the  $k$ -space data of individual slices from the collapsed slice data. Thus, for the 3-fold slice-accelerated acquisition, three separate sets of GRAPPA kernels are fitted and applied. During the GRAPPA kernels estimation, the pre-scan calibration data, acquired one slice at a time, is summed to create a synthesized collapsed dataset. A GRAPPA kernel set is then calculated for each of the slices, to best estimate the individual slice pre-scan data from the synthesized collapsed dataset. It was shown in [21] that under normal brain imaging conditions were sufficient image structures exist, slice-GRAPPA fitting

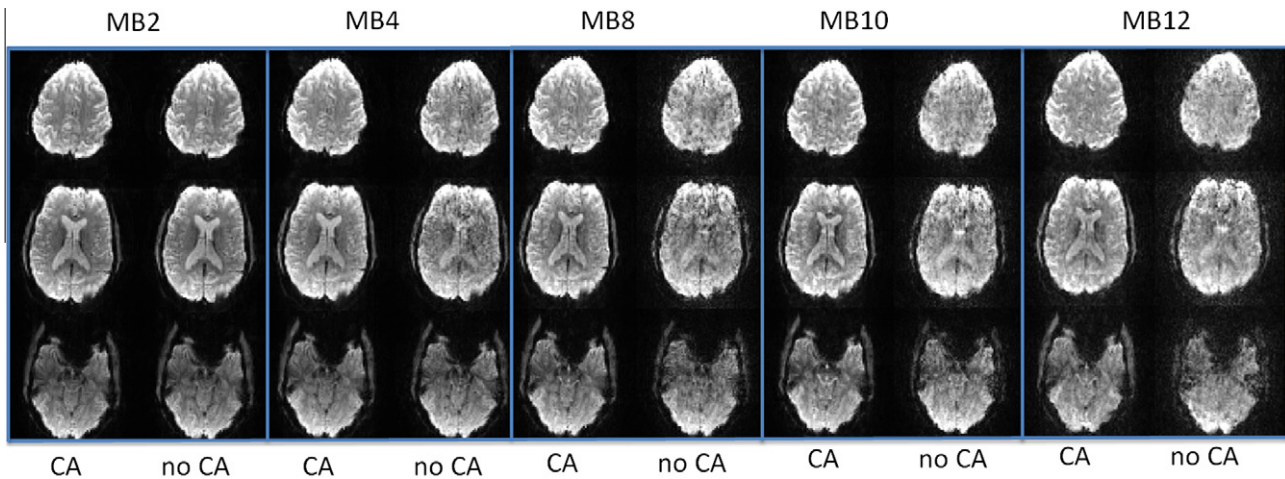


**Fig. 7.** Comparison of SMS EPI with blipped-CAIPI controlled aliasing (CA) and without (no CA). At low acceleration of MB2 images look about the same but at MB-4 and higher MB-8 there is severe artifact with no CA and higher g-factor in images. Each column shows 3 of 36–40 images acquired in separate scan of the brain with all parameters except MB-factor held constant: TR = 2 s, TE = 36 ms, 70°, isotropic 2.5 mm voxels. The actual minimum achievable scan time of the brain could be reduced by shortening TR from the time required for normal EPI  $\sim 3$  s divided by MB down to  $\sim 250$  ms at MB-12. Shorter TR requires reducing flip angle to reduce SAR, which also changes image contrast. (provided by Liyong Chen, Steen Moeller and David Feinberg).

algorithm permits the resulting kernels to utilize fixed coil sensitivities information to successfully un-alias the slices. However, in phantoms with no or limited structure, the fitting algorithm tends to cause the kernels to rely on both the underlying image signal of the pre-scan data and the coil sensitivities to un-alias the slices. Since the underlying image signal can change from one TR to the next (due to e.g. diffusion encoding or phase drift) the unaliasing performance of such algorithm tends to be quite poor in such cases when there is little structure in the image. Detailed description and analysis of the slice-GRAPPA algorithm can be found in [21].

Ongoing studies seem to indicate that the use of high slice and in-plane accelerations leads to an increased sensitivity to physiological noise for diffusion imaging. Of particular importance for diffusion measurement is the concurrent sensitivity to velocity phase shifts [17] from brain pumping action and CSF motion [42]. These vascular driven motions cause image artifacts, particularly in lower central brain regions. The constrained optimization technique in calculating slice-GRAPPA kernels as proposed by Cauley et al. [43] and its variants being investigated can significantly reduce the signal leakage between the simultaneously excited slices. As a result, these new algorithms seem to have the ability to mitigate the strong dip in tSNR in the lower central brain regions. This is an important and active area of research, which will allow for more robust use of SMS acquisitions at high acceleration factors.

The blipped-CAIPI modification of SMS EPI acquisition has allowed for a dramatic increase in the slice acceleration factor from MB-3 to MB-12. This has been achieved by spreading the voxel aliasing pattern to both the slice as well as the in-plane phase encoding directions, thereby increasing the distance between the aliasing voxels to make better use of the spatial variation of the coil sensitivities in teasing apart the aliased voxels. Nonetheless, when parallel imaging in-plane acceleration is used in combination with slice acceleration, the ability for the blipped-CAIPI sequence to spread the aliasing is constrained by the aliasing that is already in place in the image phase encoding direction. Therefore, the achievable slice acceleration factor at acceptable g-factor and image artifact levels is more limited. Recently, the wave-CAIPI sequence was introduced [44] as a way to try to address this issue. With this sequence, additional sinusoidal  $G_p$  and  $G_s$  gradients are applied during the acquisition of each  $k_r$  readout line of a simultaneous multi-slice acquisition. The application of these extra

gradients allows for the spreading of the aliasing voxels into the read direction, in addition to the PE and slice directions. It was shown in a FLASH acquisition that, with such technique, a  $3 \times 3$  acceleration factor (PE  $\times$  slice) can be achieved at almost no g-factor penalty using a 32 channel head coil at 3 T. The application of such technique to rapid SMS-EPI acquisition is a promising avenue, but will require good characterization of the gradient systems for accurate reconstruction.

## 2. Discussion

### 2.1. RF power limitations

RF heating is the major potential problem and serious physiologic limitation of the SMS technique with the relatively high energy requirement of the MB RF pulses leading to high Specific Absorption Rate (SAR). The peak power of a multi-band RF pulse scales with the square of the number of simultaneously excited slices. This quadratic increase in peak power is partially mitigated in GE-EPI, where the excitation flip angle is typically reduced to follow Ernst angle at short TRs used for fMRI. However, for SE-EPI which requires multiband 180° refocusing as used for diffusion imaging, the quadratic increase in peak power can easily cause the SAR to exceed safety limits as does the greater power requirements of ultra-high field 7 T imaging [24]. The peak power can be reduced by lengthening the duration of the RF pulse and by employing the VERSE algorithm [45]. The lengthened pulses increase the TE and the TR, and can cause degradation in the slice profile for off resonance spins. Similarly, the VERSE pulse also degrades slice profiles for off-resonance spins. The current use of VERSE to reduce RF energy is already close to its limits for refocusing pulses in a typical diffusion imaging sequence at 3 T with MB = 3 or 4. New alternative RF pulse designs with lowered RF energy requirement will be needed to achieve higher MB factors for SE-EPI based fMRI and diffusion imaging at 7 T. Note that for spin-echo sequence, the optimal SNR is achieved at 1.25T1 and a higher MB factor is typically not useful in most SE-EPI imaging protocols.

The recently proposed “power independent of number of slices” (PINS) RF pulses can be used to significantly reduce SAR [46]. This technique relies on the use of a comb function to modulate the rf pulse and encode a periodic distribution of excitation. This results in a simultaneous multi-slice excitation with power characteristic

that is nearly independent of the number of simultaneously excited slices. The PINS method was successfully used in a typically SAR intensive multiband spin echo resting state fMRI acquisition at 7 T [46–48]. We note that the periodic function that defines excitation of slices in PINS may have less well defined slice profile. While axial oriented images would have slices extending into low coil sensitivity regions in the neck, with excitation in the sagittal orientation, signal is limited by the head–air interfaces. The combined use of PINS pulse and selective excitation pulses has been proposed to circumvent this limitation [47]. An alternative approach in reducing rf power is by specifying a different rf phase for each of the frequency modulated rf waveforms in the multiband pulse [49] following earlier work on phase shifted multiband pulses [50,51]. It was shown that, with this technique, the rf peak power can be reduced by more than a factor of two at high MB factors. However, this method does not reduce the total energy of the RF pulse and therefore it is not clear to what extent SAR is reduced. Future development is still necessary to further reduce power requirement of MB pulses. The use of parallel transmit can potentially offer a solution, whereby different rows of transmit coils in a transmit array are used to excite different slices in a simultaneous multi-slice excitation. With such technique, each row of transmit coil will excite a subset of slices and hence required much lower power.

## 2.2. Gradient limitations

For human imaging, the gradient slew rate is limited for safety reasons to avoid physiological stimulation including peripheral nerve stimulation (PNS) and cardiac stimulation. Gradient slew rate of EPI read gradient switching and of large amplitude gradients used for diffusion encoding must both be limited. Nearly all MRI scanners are built with long gradient coils for whole body imaging and have slew rates limited to  $200 \text{ T m}^{-1} \text{ s}^{-1}$ . Smaller head only insertable gradient coils which do not cover the thorax can use twice the slew rate,  $400 \text{ T m}^{-1} \text{ s}^{-1}$ . A slower slew rate increases the echo spacing and hence increases image distortion and total  $T_2^*$  decay in the resulting longer echo trains. To some extent in-plane parallel imaging can mitigate these effects by reducing the effective echo spacing and the echo train length. However, when in-plane parallel imaging is used in combination with slice parallel imaging in SMS acquisition, the combined acceleration factor is the product of the acceleration factors and the g-factor increases significantly. This increases quite rapidly, thereby limiting the achievable MB factor. Improvement in image distortion correction and/or control aliasing algorithms is needed to allow for rapid EPI acquisition with high MB factor that produces largely distortion free images. Development of shorter gradient coils to cover primarily the head region therefore would substantially improve SMS-EPI by providing faster gradient switching to shorten echo trains and in turn reduce susceptibility based image artifacts, distortions and shorten TE.

## 2.3. High field imaging

High field imaging is used to study the brain with greater spatial resolution and with increased BOLD contrast due to the susceptibility contrast mechanisms that are field dependent. At higher field strength imaging is performed with thinner slices, Fig. 8, to reduce signal drop-out in the image caused by the increased intravoxel dephasing due to increased  $B_0$  inhomogeneity. However, the use of thinner images requires proportionally larger number of images for whole brain coverage in fMRI, which in turn increases the scan time. To overcome this problem, the earliest 7 T studies [24] achieved a fourfold increase in the number of images per TR using SMS EPI acceleration.

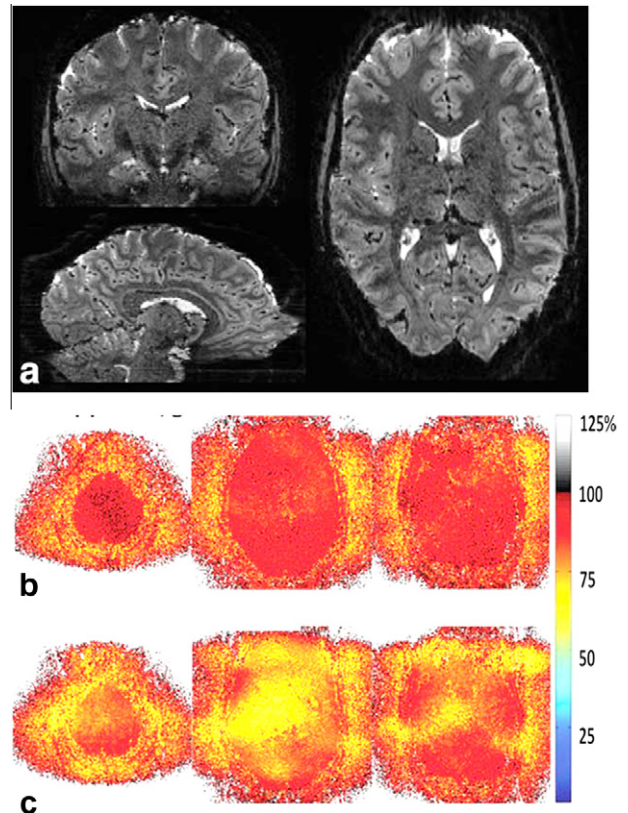


**Fig. 8.** Simultaneous multi-slice EPI at 1-mm isotropic resolution, imaging whole-brain GRE-EPI blipped-CAIPI acquisition at 7 Tesla with 3 slice (MB-3) and 2 in-plane acceleration (TR = 2.88 s). (a) Coronal, sagittal, and axial views of the unaliased 3D volume. (b and c) Corresponding 1/g map of a representative slice group for blipped-CAIPI and non-blipped acquisition, respectively. Adapted from [33].

The biological heating from multiband rf pulses increases greatly with field strength as the rf power increases quadratically with magnetic field strength. The ability of rf pulse lengthening and VERSE algorithm to mitigate the SAR heating problem is not sufficient for the use of high MB factors in SE EPI acquisitions at 7 T. The recent application of PINS pulse to SE EPI reduced SAR at 7 T and appears to be a very useful SAR reduction approach at these higher fields [47,48]. The SIR SE EPI sequence may have an advantage of reduced SAR at ultra-high field imaging as the refocusing pulse can cover two or more adjacent slices without using MB pulses which have much greater peak power [12]. The inherent bandwidth difference between excitation and refocusing pulses of SIR SE EPI causes the lipid signal not to be refocused at 7 T which obviates the need of lipid suppression pulses and this further reduces SAR.

## 2.4. Diffusion image optimization

Regarding sequence optimizations, the optimal TR for SE-EPI based diffusion imaging that maximizes SNR per unit time is  $\sim 1.25T_1$  [52,53]. Nonetheless, when compare to this optimal TR, the SNR per unit time of an acquisition at TR of  $2.6T_1$  is already  $\sim 90\%$  of the optimal value, while the SNR per shot at this TR is 25% larger. This significantly larger SNR per shot results in less sensitivity to the non-Gaussian noise behavior and the resulting bias in the estimation of diffusion parameters [10]. Additionally, acquisition at such TR would exhibit much smaller g-factor and image artifact penalty, since a much lower slice acceleration factor would be required. Based on this analysis, for most diffusion acquisitions,

the ideal operating TR would be around 2.5–3 s at 3 T. The typical TR for e.g. 2 mm isotropic resolution in whole brain acquisition is around 10 s. Therefore the use of MB = 3–4 is generally sufficient and blipped-CAIPI allows this to be achieved with minimal  $g$ -factor penalty in diffusion imaging, Fig. 9. However, a somewhat higher MB factor might be required when higher resolution imaging (1.5 mm or 1 mm) with longer TR used. The use of SIR might not be ideal for diffusion imaging if MB is already used. The TE increase and hence T2 signal loss from SIR can be quite significant compare to the additional SNR gain that could be achieved from further TR reduction.

Diffusion imaging is challenged by the use of strong diffusion encoding gradients for high  $b$ -values and high spatial resolution, as both substantially reduce image SNR. Higher maximum gradients allow shorter pulses for earlier TE reducing T2 signal decay in the echo train which raises SNR. In spin echo based diffusion sequence, using either the Stejskal–Tanner sequence or the twice refocused SE sequence [54], the  $b$ -value has  $b = \gamma^2 G_d^2 \delta^2 (\Delta - \delta/3)$  dependence where  $\gamma$  is the gyromagnetic ratio,  $G_d$  is the amplitude of the diffusion encoding gradient pulse where for a given  $b$ -value the maximum gradient,  $G_{max}$  reduces the gradient pulse times to shorten TE. Most commercial MRI scanners have  $G_{max}$  in the range of 30–50 mT/m peak gradient amplitudes on 1.5 T and 3 T scanners and 70 mT/m on 7 T scanners (Siemens). Stronger gradient systems for human brain imaging have recently been developed for the NIH Human Connectome Project for 3 T scanners (Skyra, Siemens); at Washington University the scanner has  $G_{max}$  of 110 mT/m and at the MGH Harvard laboratory a scanner with  $G_{max}$  of 300 mT/m for dedicated diffusion research [55]. The stronger gradients are only useful for the diffusion pulses and not for shortening the echo trains to reduce TE where the gradient switching and peak gradient amplitude of the read gradient contribute to physiological stimulation and therefore the gradient hardware system is slow rate limited to 200 mT/m/s to remain within safety guidelines. Additional reductions in diffusion data acquisition time for HARDI fiber tractography can be accomplished using more efficient sampling of the  $q$ -space coverage; i.e., compressed sensing [56–58] combined with SMS-EPI has enabled a 12-fold time reduction in Diffusion Spectrum Imaging (DSI) acquisitions [11].

### 2.5. fMRI with faster imaging

In considering optimization of imaging speed for fMRI, the potential gains in neuronal information will undoubtedly be limited by the sluggish hemodynamic response of BOLD and by delay differences in neurovascular coupling between different brain regions. Yet as shown in functional connectivity research [12,59],

task based fMRI will likely benefit from the improved statistics offered by higher sampling rates. Slice time correction procedures with their interpolation effects on temporal precision in sampling neuronal signal will to a large extent be mitigated by simultaneous timing. Another advantage of high temporal resolution is that physiological noise from cardiac and respiratory effects on periodic signal variation can be resolved and filtered from the BOLD signal. It is not clear at this time what could be the best sampling frequency, given the conventional EPI at 3 s TR samples a  $\sim 0.33$  Hz band and with faster sequences it is possible to sample  $\sim 10$  Hz capable of largely oversampling and avoid frequency aliasing of respiration and cardiac frequencies [60–62]. A tradeoff of faster sampling with less time for signal recovery using reduced TR would lead to lower SNR. However the shorter TR allows use of lower Ernst angle pulses which in turn leads to another favorable tradeoff in reducing the SAR of higher MB excitation pulses.

The use of multiplexed EPI with high MB acceleration factor to achieve very fast whole brain coverage will have challenges of higher  $g$ -factors and limitations of SAR which may require extensive changes in RF pulse designs. In these very fast TR regimes the use of 3D encoding permits much reduced SAR via the use of a single volume selective pulse rather than using multiband pulses for multi-slice 2D imaging. Very fast scanning in the realm of 100 ms TR for fMRI and functional connectivity research is also being pursued with non-Cartesian  $k$ -space trajectories in MR encephalography approaches which have evolved in efficiency from concentric shells to stack of spiral trajectories [60–62]. Using TRs of a few 100 ms there is sufficient oversampling of cardiac and respiratory frequencies in time-series fMRI studies to allow filtering of these physiological noise sources.

### 2.6. Future volume imaging

Simultaneous multi-volume rather than multi-slice imaging is one interesting direction to explore as a possible means of increasing speed and resolution and reducing SAR. The encoding of contiguous 3D slices with a conventional selective excitation pulse would have much lower SAR than a similar slice number MB pulse. Exciting only a few limited thickness 3D slabs with a MB pulse would reduce SAR compared to SMS-EPI and potentially increase slice coverage. There are two types of sequences commonly used for single-shot 3D imaging of brain. The first is the echo volume imaging (EVI) and multi-slab variants which has been utilized for fMRI [63]. While the second type, producing gradient echoes and spin-echo (GRASE) [64] is derivative of a CPMG pulse sequence with multiple gradient refocused echoes between the 180° refocusing pulses. The 3D GRASE sequence is used for brain perfusion mapping with the

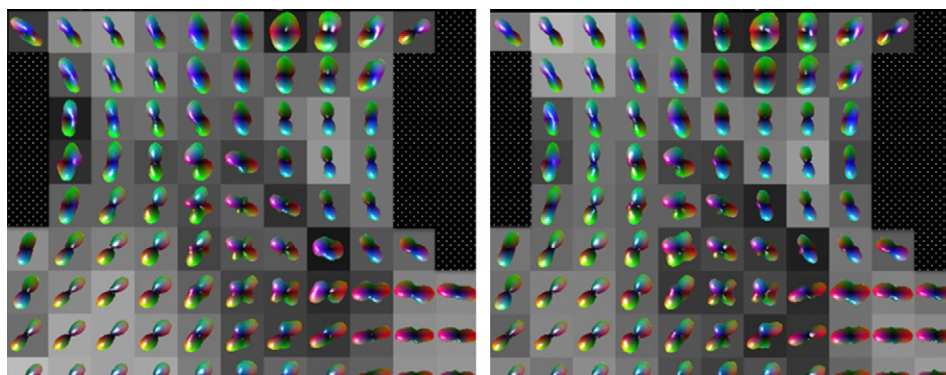


**Fig. 9.** Comparison of the general fractional isotropy (GFA) in a diffusion Q ball based orientation distribution function with a 3× faster scan time using SMS EPI (left) acquired without SMS with 2× in-plane accelerated (10 min), and (right) MB-3 SMS and 2× in-plane accelerated (3.3 min) acquisitions. Similar results are observed. Adapted from [11].

ASL technique and used for ultra-high resolution fMRI at 7 T using zoomed resolution approaches [5,8,65]. One limiting effect with longer 3D encoding sequences is slice blurring due to spin relaxation. It should be possible to greatly reduce this problem by shortening echo trains using simultaneous multi-volume excitations to maintain slice coverage; i.e., MB-2 would reduce echo train by half to reduce blurring or to a lesser extent for increased slice coverage. In addition to perfusion imaging, velocity phase imaging is the most common approach used for hemodynamic imaging for which SMS-EPI can be used to measure positions simultaneously [66] and modified with segmented sequence variants for simultaneity in physiological measurements of velocity, tissue strain and pulsatility while eliminating cardiac cycle variations by recording slices simultaneously.

### 3. Conclusion

Simultaneous multi-slice EPI achieves high speed through multiplexing image data and then extracting the images with multiple receiver systems. The resulting reduction in imaging time does not rely on reducing the echo train length,  $N$ , and therefore SMS-EPI does not incur the  $\sqrt{N}$  dependent reduction in SNR as occurs with scan time reductions from partial Fourier and in-plane parallel acceleration techniques. To fully utilize these higher achievable imaging speeds future reduction of peak power to remain within SAR limits will require further innovations in rf pulse design exemplified by the PINS pulse and potentially the use of multi-channel transmission systems. Another important requirement for EPI based brain imaging is the requisite fast gradient switching and high gradient amplitude, which must be within safety limits to avoid peripheral nerve stimulation.

Many neuroscience studies using fMRI and diffusion imaging as well as diagnostic medical imaging will likely benefit from simultaneous multi-slice technology. In addition to brain applications, diffusion imaging is commonly used for imaging the body for which large reductions in scan time should be very desirable in diagnostic radiology. The simultaneous multi-slice technique contributes to an increase in MR efficiency and allows trade-off between, scan time, SNR and spatial resolution. One promising impact will be if the faster imaging allows patients to tolerate new quantitative studies of the brain using structural and physiological metric currently requiring too much time in the scanner. The recent large increases in speed of simultaneous multi-slice imaging will facilitate the translation of basic neuroimaging research to improve mental health by providing new insights into neurological disorders.

### 4. Disclosure

David Feinberg is an employee of Advanced MRI Technologies, which is engaged in the development of magnetic resonance imaging pulse sequences. Some of the innovation and design of the pulse sequences presented in this work were done by Advanced MRI Technologies. However, this does not alter the authors adherence to all policies of the journal.

### Acknowledgement

The work was supported by grants NIH NIBIB R00EB012107, NINDS R44NS073417, the NIH Blueprint for 788 Neuroscience Research U01MH093765 the Human Connectome project. The authors thank Nikolaus Weiskopf for helpful comments on the manuscript. The authors wish to thank all their collaborators on these pulse sequences.

### References

- [1] D.C. Van Essen, M.F. Glasser, D.L. Dierker, J. Harwell, T. Coalson, Parcellations and hemispheric asymmetries of human cerebral cortex analyzed on surface-based atlases, *Cereb. Cortex* 22 (2011) 2241–2262.
- [2] V. Braitenberg, A. Schüz, *Anatomy of the Cortex: Statistics and Geometry*, Springer, 1991. p. 249.
- [3] D.C. Van Essen, K. Ugurbil, E. Auerbach, D. Barch, T.E. Behrens, R. Bucholz, A. Chang, L. Chen, M. Corbetta, S.W. Curtiss, S. Della Penna, D. Feinberg, M.F. Glasser, N. Harel, A.C. Heath, L. Larson-Prior, D. Marcus, G. Michalareas, S. Moeller, R. Oostenveld, S.E. Petersen, F. Prior, B.L. Schlaggar, S.M. Smith, A.Z. Snyder, J. Xu, E. Yacoub, The human connectome project: a data acquisition perspective, *Neuroimage* 62 (2012) 2222–2231.
- [4] C.A. Olman, N. Harel, D.A. Feinberg, S. He, P. Zhang, K. Ugurbil, E. Yacoub, Layer-specific fMRI reflects different neuronal computations at different depths in human V1, *PLoS One* 7 (2012) e32536.
- [5] J. Zimmermann, R. Goebel, F. De Martino, P.F. van de Moortele, D. Feinberg, G. Adriany, D. Chaimow, A. Shmuel, K. Ugurbil, E. Yacoub, Mapping the organization of axis of motion selective features in human area MT using high-field fMRI, *PLoS One* 6 (2011) e28716.
- [6] J.R. Polimeni, B. Fischl, D.N. Greve, L.L. Wald, Laminar analysis of 7 T BOLD using an imposed spatial activation pattern in human V1, *Neuroimage* 52 (2010) 1334–1346.
- [7] D.H. Hubel, T.N. Wiesel, Receptive fields, binocular interaction and functional architecture in the cat's visual cortex, *J. Physiol.* 160 (1962) 106–154.
- [8] E. Yacoub, N. Harel, K. Ugurbil, High-field fMRI unveils orientation columns in humans, *Proc. Natl. Acad. Sci. USA* 105 (2008) 10607–10612.
- [9] H. Johansen-Berg, M.F. Rushworth, Using diffusion imaging to study human connective anatomy, *Annu. Rev. Neurosci.* 32 (2009) 75–94.
- [10] D.K. Jones, P.J. Basser, "Squashing peanuts and smashing pumpkins": how noise distorts diffusion-weighted MR data, *Magn. Reson. Med.* 52 (2004) 979–993.
- [11] K. Setsompop, J. Cohen-Adad, B.A. Gagoski, T. Raji, A. Yendiki, B. Keil, V.J. Wedeen, L.L. Wald, Improving diffusion MRI using simultaneous multi-slice echo planar imaging, *Neuroimage* 63 (2012) 569–580.
- [12] D.A. Feinberg, S. Moeller, S.M. Smith, E. Auerbach, S. Ramanna, M. Gunther, M.F. Glasser, K.L. Miller, K. Ugurbil, E. Yacoub, Multiplexed echo planar imaging for sub-second whole brain fMRI and fast diffusion imaging, *PLoS One* 5 (2010) e15710.
- [13] P. Mansfield, Multi-planar image formation using NMR spin echoes, *J. Phys. C: Solid State Phys.* 10 (1977) L55.
- [14] P. Mansfield, A.A. Maudsley, Medical imaging by NMR, *Br. J. Radiol.* 50 (1977) 188–194.
- [15] K.K. Kwong, J.W. Belliveau, D.A. Chesler, I.E. Goldberg, R.M. Weisskoff, B.P. Poncelet, D.N. Kennedy, B.E. Hoppel, M.S. Cohen, R. Turner, et al., Dynamic magnetic resonance imaging of human brain activity during primary sensory stimulation, *Proc. Natl. Acad. Sci. USA* 89 (1992) 5675–5679.
- [16] P.A. Bandettini, E.C. Wong, R.S. Hinks, R.S. Tikofsky, J.S. Hyde, Time course EPI of human brain function during task activation, *Magn. Reson. Med.* 25 (1992) 390–397.
- [17] D.A. Feinberg, A.S. Mark, Human brain motion and cerebrospinal fluid circulation demonstrated with MR velocity imaging, *Radiology* 163 (1987) 793–799.
- [18] V.J. Wedeen, D.L. Rosene, R. Wang, G. Dai, F. Mortazavi, P. Hagmann, J.H. Kaas, W.Y. Tseng, The geometric structure of the brain fiber pathways, *Science* 335 (2012) 1628–1634.
- [19] D.A. Feinberg, J.D. Hale, J.C. Watts, L. Kaufman, A. Mark, Halving MR imaging time by conjugation: demonstration at 3.5 kG, *Radiology* 161 (1986) 527–531.
- [20] K.P. Pruessmann, M. Weiger, M.B. Scheidegger, P. Boesiger, SENSE: sensitivity encoding for fast MRI, *Magn. Reson. Med.* 42 (1999) 952–962.
- [21] M.A. Griswold, P.M. Jakob, R.M. Heidemann, M. Nittka, V. Jellus, J. Wang, B. Kiefer, A. Haase, Generalized autocalibrating partially parallel acquisitions (GRAPPA), *Magn. Reson. Med.* 47 (2002) 1202–1210.
- [22] Z.P. Liang, B. Madore, G.H. Glover, N.J. Pelc, Fast algorithms for GS-model-based image reconstruction in data-sharing Fourier imaging, *IEEE Trans. Med. Imaging* 22 (2003) 1026–1030.
- [23] T. Jaermann, G. Crelier, K.P. Pruessmann, X. Golay, T. Netsch, A.M. van Muiswinkel, S. Mori, P.C. van Zijl, A. Valavanis, S. Kollias, P. Boesiger, SENSE-DTI at 3 T, *Magn. Reson. Med.* 51 (2004) 230–236.
- [24] S. Moeller, E. Yacoub, C.A. Olman, E. Auerbach, J. Strupp, N. Harel, K. Ugurbil, Multiband multislice GE-EPI at 7 Tesla, with 16-fold acceleration using partial parallel imaging with application to high spatial and temporal whole-brain fMRI, *Magn. Reson. Med.* 63 (2010) 1144–1153.
- [25] D.J. Larkman, J.V. Hajnal, A.H. Herlihy, G.A. Coutts, I.R. Young, G. Ehnholm, Use of multicoil arrays for separation of signal from multiple slices simultaneously excited, *J. Magn. Reson. Imaging* (2001) 313–317.
- [26] D.A. Feinberg, T.G. Reese, V.J. Wedeen, Simultaneous echo refocusing in EPI, *Magn. Reson. Med.* 48 (2002) 1–5.
- [27] P.R. Harvey, P. Mansfield, Echo-volumar imaging (EVI) at 0.5 T: first whole-body volunteer studies, *Magn. Reson. Med.* 35 (1996) 80–88.
- [28] K.P. Pruessmann, M. Weiger, P. Bornert, P. Boesiger, Advances in sensitivity encoding with arbitrary  $k$ -space trajectories, *Magn. Reson. Med.* 46 (2001) 638–651.
- [29] R.G. Nunes, J.V. Hajnal, X. Golay, D.J. Larkman, Simultaneous slice excitation and reconstruction for single shot EPI, in: *Proceedings of the 14th Annual Meeting of ISMRM*, Seattle, Washington, 2006, p. 293.

- [30] M.N. Paley, K.J. Lee, J.M. Wild, P.D. Griffiths, E.H. Whitby, Simultaneous parallel inclined readout image technique, *Magn. Reson. Imaging* 24 (2006) 557–562.
- [31] M. Blaimer, F.A. Breuer, N. Seiberlich, M.F. Mueller, R.M. Heidemann, V. Jellus, G. Wiggins, L.L. Wald, M.A. Griswold, P.M. Jakob, Accelerated volumetric MRI with a SENSE/GRAPPA combination, *J. Magn. Reson. Imaging* 24 (2006) 444–450.
- [32] T.G. Reese, T. Benner, R. Wang, D.A. Feinberg, V.J. Wedeen, Halving imaging time of whole brain diffusion spectrum imaging and diffusion tractography using simultaneous image refocusing in EPI, *J. Magn. Reson. Imaging* 29 (2009) 517–522.
- [33] K. Setsompop, B.A. Gagoski, J.R. Polimeni, T. Witzel, V.J. Wedeen, L.L. Wald, Blipped-controlled aliasing in parallel imaging for simultaneous multislice echo planar imaging with reduced g-factor penalty, *Magn. Reson. Med.* 67 (2012) 1210–1224.
- [34] A. Jesmanowicz, A.S. Nencka, S.J. Li, J.S. Hyde, Two-axis acceleration of functional connectivity magnetic resonance imaging by parallel excitation of phase-tagged slices and half k-space acceleration, *Brain Connect* 1 (2011) 81–90.
- [35] R.M. Mersereau, The processing of hexagonally sampled two dimensional signals, *Proc. IEEE* 67 (1979) 930–949.
- [36] J.C. Ehrhardt, MR data acquisition and reconstruction using efficient sampling schemes, *IEEE Trans. Med. Imaging* 9 (1990) 305–309.
- [37] J.C. Ehrhardt, Hexagonal fast Fourier transform with rectangular output, *IEEE Trans. Signal Process.* 41 (1993) 1469–1472.
- [38] J. Tsao, S. Kozerke, P. Boesiger, K.P. Pruessmann, Optimizing spatiotemporal sampling for k-t BLAST and k-t SENSE: application to high-resolution real-time cardiac steady-state free precession, *Magn. Reson. Med.* 53 (2005) 1372–1382.
- [39] F.A. Breuer, M. Blaimer, R.M. Heidemann, M.F. Mueller, M.A. Griswold, P.M. Jakob, Controlled aliasing in parallel imaging results in higher acceleration (CAIPIRINHA) for multi-slice imaging, *Magn. Reson. Med.* 53 (2005) 684–691.
- [40] J.B. Weaver, Simultaneous multislice acquisition of MR images, *Magn. Reson. Med.* 8 (1988) 275–284.
- [41] J. Xu, S. Moeller, J. Strupp, E.J. Auerbach, L. Chen, D.A. Feinberg, K. Ugurbil, E. Yacoub, Highly Accelerated Whole Brain Imaging Using Aligned-Blipped-Controlled-Aliasing Multiband EPI, ISMRM 20th Annual Meeting, ISMRM, 2012.
- [42] B.P. Poncet, V.J. Wedeen, R.M. Weisskoff, M.S. Cohen, Brain parenchyma motion: measurement with cine echo-planar MR imaging, *Radiology* 185 (1992) 645–651.
- [43] S.E. Cauley, K. Setsompop, J.R. Polimeni, L.L. Wald, Inter-Slice Artifact Reduction for Slice-GRAPPA Reconstruction of Simultaneous Multi-Slice (SMS) Acquisitions, Sequences: New Acquisition Strategies & Applications, ISMRM, 2012, p. 2543.
- [44] K. Setsompop, B.A. Gagoski, J.R. Polimeni, L.L. Wald, Wave-CAIPIRINHA: A Method for Reducing g-factors in Highly Accelerated 3D Acquisitions, ISMRM 19th Annual Meeting, ISMRM, 2011, p. 0478.
- [45] S. Conolly, D. Nishimura, A. Macovski, G. Glover, Variable-rate selective excitation, *J. Magn. Reson.* 78 (1988) 440–458.
- [46] D.G. Norris, P.J. Koopmans, R. Boyacioglu, M. Barth, Power Independent of Number of Slices (PINS) radiofrequency pulses for low-power simultaneous multislice excitation, *Magn. Reson. Med.* 66 (2011) 1234–1240.
- [47] P.J. Koopmans, R. Boyacioglu, M. Barth, D.G. Norris, Simultaneous multislice inversion contrast imaging using power independent of the number of slices (PINS) and delays alternating with nutation for tailored excitation (DANTE) radio frequency pulses, *Magn. Reson. Med.* (2012). <http://dx.doi.org/10.1002/mrm.24402> [Epub].
- [48] P.J. Koopmans, R. Boyacioglu, M. Barth, D.G. Norris, Whole brain, high resolution spin-echo resting state fMRI using PINS multiplexing at 7 T, *Neuroimage* 62 (2012) 1939–1946.
- [49] E. Wong, Optimized Phase Schedules for Minimizing Peak RF Power in Simultaneous Multi-Slice RF Excitation Pulses, ISMRM 20th Annual Meeting, ISMRM, 2012, p. 2209.
- [50] G. Johnson, E.X. Wu, S.K. Hilal, Optimized phase scrambling for RF phase encoding, *J. Magn. Reson. B* 103 (1994) 59–63.
- [51] J. Hennig, Chemical shift imaging with phase-encoding RF pulses, *Magn. Reson. Med.* 25 (1992) 289–298.
- [52] M.A. Bernstein, K.F. King, X.J. Zhou, *Handbook of MRI Pulse Sequences*, Elsevier, Burlington, MA, 2004.
- [53] G. Johnson, Y.Z. Wadghiri, D.H. Turnbull, 2D multislice and 3D MRI sequences are often equally sensitive, *Magn. Reson. Med.* 41 (1999) 824–828.
- [54] D.A. Feinberg, P.D. Jakob, Tissue perfusion in humans studied by Fourier velocity distribution, line scan, and echo-planar imaging, *Magn. Reson. Med.* 16 (1990) 280–293.
- [55] R.E. Kimmlingen, Eva, Dietz, Peter, Kreher, Sabrina, Schuster, Johann, Riegler, Jörg, Matschl, Volker, Schnetter, Volker, Schmidt, Andreas, Lenz, Helmut, Mustafa, Ernst, Fischer, Daniel, Potthast, Andreas, Kreisler, Ludwig, Eberler, Michael, Hebrank, Franz, Thein, Herbert, Heberlein, Keith, Hoecht, Philipp, Witzel, Thomas, Tisdall, Dylan, Xu, Junqian, Yacoub, Essa, Adriany, Gregor, Auerbach, Edward, Moeller, Steen, Feinberg, David, Lehne, Dietmar, Wald, L. Lawrence, Rosen, Bruce, Ugurbil, Kamil, Essen, David van, Wedeen, Van, Schmitt, Franz, Concept and Realization of High Strength Gradients for the Human Connectome Project, ISMRM 20th Annual Meeting, ISMRM, 2012, p. 0696.
- [56] M.I. Menzel, E.T. Tan, K. Khare, J.I. Sperl, K.F. King, X. Tao, C.J. Hardy, L. Marinelli, Accelerated diffusion spectrum imaging in the human brain using compressed sensing, *Magn. Reson. Med.* 66 (2011) 1226–1233.
- [57] M. Lustig, D. Donoho, J.M. Pauly, Sparse MRI: the application of compressed sensing for rapid MR imaging, *Magn. Reson. Med.* 58 (2007) 1182–1195.
- [58] B. Bilgic, K. Setsompop, J. Cohen-Adad, A. Yendiki, L.L. Wald, E. Adalsteinsson, Accelerated Diffusion Spectrum Imaging with Compressed Sensing using Adaptive Dictionaries, MACCAI, ISMRM, 2012.
- [59] S.M. Smith, K.L. Miller, S. Moeller, J. Xu, E.J. Auerbach, M.W. Woolrich, C.F. Beckmann, M. Jenkinson, J. Andersson, M.F. Glasser, D.C. Van Essen, D.A. Feinberg, E.S. Yacoub, K. Ugurbil, Temporally-independent functional modes of spontaneous brain activity, *Proc. Natl. Acad. Sci. USA* 109 (2012) 3131–3136.
- [60] J. Asslender, M. Reisert, B. Zahneisen, T. Hugger, J. Hennig, MR-Encephalography using a Spherical Stack of Spirals Trajectory, ISMRM 20th Annual Meeting, ISMRM, 2012, p. 2426.
- [61] B. Zahneisen, T. Hugger, K.J. Lee, P. LeVan, M. Reisert, H.L. Lee, J. Asslender, M. Zaitsev, J. Hennig, Single shot concentric shells trajectories for ultra fast fMRI, *Magn. Reson. Med.* 68 (2012) 484–494.
- [62] F.H. Lin, T. Witzel, J.B. Mandeville, J.R. Polimeni, T.A. Zeffiro, D.N. Greve, G. Wiggins, L.L. Wald, J.W. Belliveau, Event-related single-shot volumetric functional magnetic resonance inverse imaging of visual processing, *Neuroimage* 42 (2008) 230–247.
- [63] S. Posse, E. Ackley, R. Mutihac, J. Rick, M. Shane, C. Murray-Kreznar, M. Zaitsev, O. Speck, Enhancement of temporal resolution and BOLD sensitivity in real-time fMRI using multi-slab echo-volumar imaging, *Neuroimage* 61 (2012) 115–130.
- [64] D.A. Feinberg, K. Oshio, GRASE (gradient- and spin-echo) MR imaging: a new fast clinical imaging technique, *Radiology* 181 (1991) 597–602.
- [65] D. Feinberg, N. Harel, S. Ramanna, K. Ugurbil, E. Yacoub, Sub-Millimeter Single-Shot 3D GRASE with Inner Volume Selection for T2 Weighted FMRI Applications at 7 Tesla, ISMRM 16th Annual Meeting, ISMRM, 2008, p. 2373.
- [66] D.A. Feinberg, L. Chen, A. Vu, Multiband Velocity EPI ISMRM 20th Annual Meeting, ISMRM, 2012, p. 2499.
- [67] S. Ramanna, V. Deshpande, D. Feinberg, SIR-EPI Diffusion Imaging for 3-Fold Faster Scan Time to Enable Trade-Offs in Slice Coverage and Gradient Duty Cycle Reduction, ISMRM Annual Meeting, 2010, p. 1623.